A Journal of the Gesellschaft Deutscher Chemiker

Angewandte International Edition Chemie

GDCh

www.angewandte.org

Accepted Article

Title: Macroscale Chemotaxis from a Swarm of Bacteria-Mimicking Nanoswimmers

Authors: Qiang He, Yuxing Ji, Xiankun Lin, Zhiguang Wu, Yingjie Wu, and Wei Gao

To be cited as: *Angew. Chem. Int. Ed.* 10.1002/anie.201907733
Angew. Chem. 10.1002/ange.201907733

Link to VoR: http://dx.doi.org/10.1002/anie.201907733
http://dx.doi.org/10.1002/ange.201907733

WILEY-VCH

10.1002/anie.201907733

WILEY-VCH

COMMUNICATION

Macroscale Chemotaxis from a Swarm of Bacteria-Mimicking Nanoswimmers

Yuxing Ji,[a] Xiankun Lin,[a] Zhiguang Wu,[a] Yingjie Wu,[a] Wei Gao,[b] and Qiang He [a]

Abstract: Inspired by the dynamics of bacterial swarming, we report a swarm of polymer-brush-grafted glucose powered Janus gold nanoswimmers with a positive macroscale chemotactic behavior. These nanoswimmers are prepared through the grafting of polymer brushes onto one side of gold nanoparticles, following by the functionalization of glucose oxidase on the other side. The resulting polymer-brush-functionalized Janus gold nanoswimmers exhibit the efficient propulsion with a velocity of up to ~120 body lengths s^{-1} in the presence of glucose fuels. The comparative analysis of their kinematic behavior reveals that the grafted polymer brushes significantly improve the translational diffusion of Janus gold nanoswimmers. Particularly, these bacteria-mimicking Janus gold nanoswimmers display a collectively chemotactic motion along the concentration gradient of a glucose resource, which could be observed at the macroscale. Such a swarm of bacteria-mimicking biocatalytic nanoswimmers exhibiting a positive macroscale chemotaxis represents exciting progress for various biomedical applications.

Nature provides an unlimited inspiration source for researchers in their efforts to develop artificial architectures that mimic the structure and function of biological systems.[1] As an example, various bacteria such as *E.coli*., perform efficient propulsion in aqueous media by the transformation of chemical energy into mechanical movement. More importantly, bacterial swarms are able to autonomously swim toward to the nutrition sources along their concentration gradients (so-called chemotaxis), leading to a collective migration of bacteria at the macroscale.[2] Their swarming behavior has stimulated the inspiration to develop versatile synthetic micro/nanoswimmers with mobility and chemotaxis, which represents one of the most promising yet challenging tasks in nanotechnology.[3] As a result, diverse types of micro-/nanoswimmers have been developed for performing various task ranging from individual propulsion to the swarm motion.[4] However, pioneering studies have mainly focused on propulsion by integrating the natural bacteria with the synthetic micro/nanoparticles. For instance, the therapeutic cargo-loaded bacteria can be used to actively transport drugs toward targeted regions.[5]

Recently a significant number of chemically powered synthetic micro-/nanoswimmers utilizing catalytic decomposition of various fuels including hydrogen peroxide,[6] bromine/iodine,[7] acidic/basic substances,[8] and hydrazine,[9] has been described. To better mimic from the motile function of various biomolecules and organisms, substantial efforts have also been focused on the use of natural enzymes to power micro- and nanoswimmers because of their biocompatibility and variable enzyme/fuel combinations.[10] However, the study of enzyme-powered micro- and nanoswimmers is still in an early stage and the key parameters affecting their kinematic behavior are not completely revealed. For instance, the directional motion of enzyme-powered nanoswimmers is dramatically limited to the strong rotational diffusion with the decreasing sizes. Understanding the influence of the swimmers nanoarchitectures on the symmetry breaking and the increasing translational motion is still a challenging issue.

In this study, we develop the polymer brush-grafted glucose oxidase (GOx)-functionalized Janus gold (PB@JAu@GOx) nanoswimmers powered by the catalytic decomposition of glucose fuels, and also their positively collective chemotaxis at the macroscale.[11] The polymer brushes are grafted onto one side of gold nanoparticles (AuNPs) through a surface-initiated atom transfer radical polymerization (SI-ATRP) method, and GOx molecules are covalently immobilized onto the other side of AuNPs. The GOx molecules on the PB@JAu@GOx nanoswimmers catalytically decompose the glucose fuel into gluconic acid, leading to active motion (i.e. self-diffusiophoresis).[12] The grafted polymer brushes significantly improve the translational diffusion of these nanoswimmers, in contrast with those GOx-functionalized Janus Au nanoswimmers without the modification of polymer brushes. In analogy to natural bacteria, such PB@JAu@GOx nanoswimmers are able to autonomously move toward the glucose sources, indicating a collectively positive chemotaxis that can be observed at the macroscale. These results verify the unique functions and robustness of the bacteria-mimicking nanoswimmers, which represents considerable promise for diverse applications.

The fabrication process of the bacteria-mimicking nanoswimmers consisting of AuNPs, a model water-soluble polymer brush, poly(*N*-isopropylacrylamide) (PNIPAM) brush, and glucose oxidase (GOx), was schematically illustrated in Figure 1A. Briefly, citrate-stabilized AuNPs were adsorbed onto the 3-aminopropyl-trimethoxysilane coated silica microspheres (ATPES-SiO_2, ~2 μm) and then a SI-ATRP initiator, bis[2-(2-bromoisobutyryloxy)undecyl] disulfide (DTBU), was modified onto the exposed surface of AuNPs. Next, the DTBU-modified Janus AuNPs were functionalized with PNIPAM brush through SI-ATRP according to our previously reported method,[13] and then the resulting nanoswimmers were obtained after HF etching. The as-prepared PNIPAM brush functionalized Janus AuNPs were entitled as PNIPAM@JAu. Finally, the GOx was covalently bounded onto the other side of PNIPAM@JAu nanoparticles, which was denoted as PNIPAM@JAu@GOx nanoswimmers.

The scanning electron microscopy (SEM) image in Figure 1B shows that the citrate-stabilized AuNPs were uniformly adsorbed onto the surface of ATPES-SiO_2. The transmission electron microscopy (TEM) image in Figure 1C exhibits that the polymer brushes with a thickness of ~20 nm were successfully grafted

[a] Y. X. Ji, Dr. X. K. Lin, Dr. Z. G. Wu, Dr. Y. J. Wu, Prof. Q. He
Key Laboratory of Microsystems and Microstructures Manufacturing (Ministry of Education), School of Chemistry and Chemical Engineering, Harbin Institute of Technology, Yi kuang jie 2, Harbin 150080, China
[b] Prof. W. Gao,
Division of Engineering and Applied Science, California Institute of Technology, 1200 East California Boulevard, Pasadena, California 91125, United States
[*] Y. Ji and X. Lin contributed to this work equally.

Supporting information for this article is given via a link at the end of the document.

10.1002/anie.201907733

WILEY-VCH

COMMUNICATION

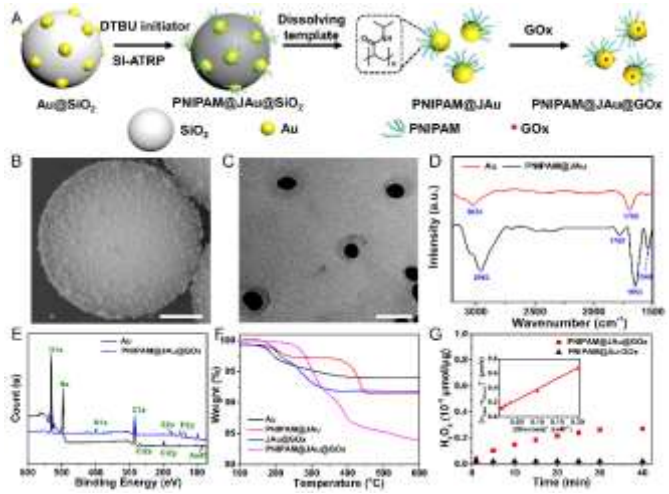

Figure 1. Fabrication and characteriaztion of PNIPAM@JAu@GOx nanoswimmers. (A) Schematic fabrication of the PNIPAM@JAu@GOx nanoswimmers. (B) Scanning electron microscopy (SEM) image of the AuNPs adsorbed on the surface of silica microparticles. Scale bar, 500 nm. (C) Transmission electron microscopy (TEM) image of the as-prepared PNIPAM@JAu nanoswimmers. Scale bar, 50 nm. (D) Fourier transform infrared (FTIR) spectra of AuNPs and PNIPAM@JAu nanoswimmers. (E) X-ray photoelectron spectroscopy (XPS) of AuNPs and PNIPAM@JAu@GOx nanoswimmers. (F) Thermogravimetric analysis (TGA) of AuNPs, PNIPAM@JAuNPs, JAu@GOx NPs, and PNIPAM@JAu@GOx nanoswimmers. (G) The catalytic activity of GOx molecules on the PNIPAM@JAu@GOx nanoswimmers and PNIPAM@Au-GOx. Inset: Michaelis–Menten steady-state kinetics of PNIPAM@JAu@GOx nanoswimmers.

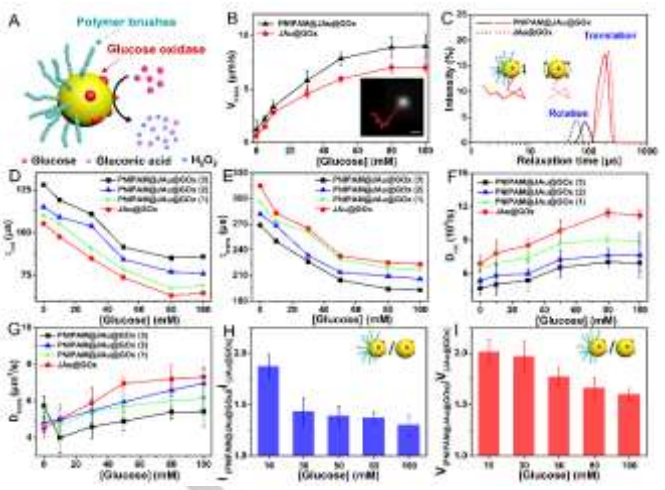

Figure 2. Characterization of the propulsion of PNIPAM@JAu@GOx nanoswimmers. (A) Scheme of the motion of PNIPAM@JAu@GOx nanoswimmers in glucose solutions. (B) Dependence of the velocity of PNIPAM@JAu@GOx and JAu@GOx nanoswimmers upon glucose concentration. The inset illustrates the propulsion of PNIPAM@JAu@GOx nanoswimmers observed by using dark-field optical microscopy. Scale bar, 2 μm. (C) Relaxation times curve of PNIPAM@JAu@GOx and JAu@GOx nanoswimmers under 100 mM glucose measued by dynamic light scattering (DLS). (D) Rotational and (E) translational diffusion relaxation times of the PNIPAM@JAu@GOx(1, 2, and 3) and JAu@GOx nanoswimmers in different concentration of glucose. (F) Rotational and (G) translational diffusion coefficient of PNIPAM@JAu@GOx (1, 2, and 3) and JAu@GOx nanoswimmers upon various concentration of glucose. (H) The ratio of average ballistic swimming length/persistence *l* and (I) velocity of PNIPAM@JAu@GOx nanoswimmers to the velocity of JAu@GOx nanoswimmers. PNIPAM@JAu@GOx(1), (2), and (3) present the PNIPAM@JAu@GOx nanoswimmers with polymerization time of 1 h, 3 h, and 6 h, respectively.

onto the one side of AuNPs with a diameter of ~25.0 ± 1.7 nm (Figure S1). Also, the zeta potential of the AuNPs changed from -34.1 mV to -15.4 mV upon the coating of PNIPAM brushes (Figure S2). The gel permeation chromatography (GPC) measurement shows that the polymer brushes had an average molecular weight of ~25 kDa and a polydispersity index (PDI) of 1.2. Fourier transform infrared spectra (FTIR) in Figure 1D shows that the characteristic peaks at 2962 cm^{-1} was corresponding to the asymmetric stretching vibration of CH_3. The peaks at 1653 and 1548 cm^{-1} were assigned to the secondary amide C=O stretching peaks. X-ray photoelectron spectroscopy (XPS) of the PNIPAM@JAu@GOx nanoswimmers in Figure 1E and Figure S3 shows that the appearance of N 1s at 399.0 eV and P 2p at 130.6 eV represents the existence of PNIPAM brushes and GOx molecules. To further establish a clear molecular profile of the PNIPAM@JAu@GOx nanoswimmers, a home-built stochastically optical reconstruction microscopy (STORM) was employed according to the previous report [14]. Briefly, the GOx was labeled with a NHS-functionalized fluorescence dye, NHS-Alexa fluor 647 (AF647), and then the PNIPAM@JAu@GOx-AF647 swimmers were observed by STORM. Figures S4A and S4B indicate the appearance of the green fluorescence dots and the green fluorescence circles before and after the nanoswimmers were adsorbed onto the silica microparticles, respectively. By comparison, no green fluorescence was observed in the absence of GOx-AF647 (Figures S4C and S4D). Similarly, the fluorescence spectra of various particles show identical results with the above STORM observation (Figure S4E). These results confirm the successful immobilization of GOx onto the nanoswimmers. Unfortunately, the STORM could not still recognize the asymmetric polymer corona and clear GOx picture of the nanoswimmers. In view of this, thermogravimetric analysis (TGA) of the PNIPAM@JAu@GOx nanoswimmers was conducted. The TGA curves indicate the percentage of PNIPAM and GOx on the PNIPAM@JAu@GOx nanoswimmers is ~9.2 wt% and ~5.9 wt%, respectively (Figure 1F and Table S1). By comparison of the amount of polymer brushes and GOx on the different particles, it can be seen that the amount of the adsorbed GOx on the PNIPAM@JAu@GOx nanoswimmers (about 3.4 GOx on each nanoswimmer) is roughly half of that on the AuNPs. In a control experiment, the TGA results demonstrate that the GOx was almost adsorbed onto the polymer brush fully coated AuNPs (PNIPAM@Au) at room temperature (Figure S5 and Table S1). Note that the high GOx concentration was applied in all experiments so that the exposed area of the AuNPs could be fully covered by GOx. These results demonstrate the asymmetric polymer corona and clear GOx picture of the nanoswimmers.

Furthermore, we assessed the biocatalytic activity of GOx molecules on the nanoswimmers using the enzyme detection assay following the published protocol.[11] Figure 1G shows that the concentration of hydrogen peroxide (H_2O_2) generated from catalytic decomposition of glucoses by GOx gradually increased upon the addition of 4 mg nanoswimmers into 3 mL of 15 mM glucose solution, suggesting that the activity of the immobilized GOx molecules was still maintained. The inset shows that the Michaelis-Menten steady-state kinetics linearly fits as an

10.1002/anie.201907733

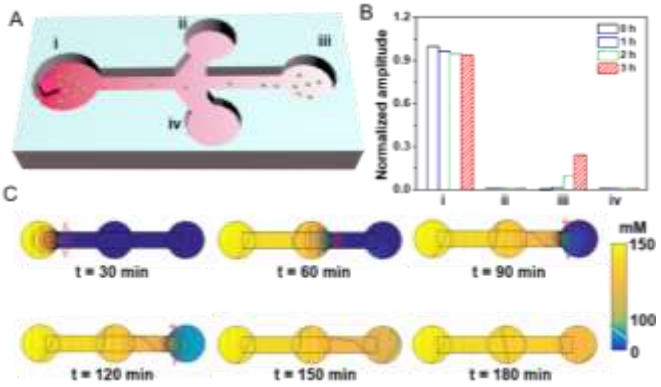

Figure 3. Positive chemotactic movement of bacteria-mimicking PNIPAM@JAu@GOx nanoswimmers at the macroscale. (A) Schematic of the horizontal chemotaxis of the nanoswimmers toward an agarose gel containing glucose as glucose source in a microfluidic channel. A time t = 0, the 15 mM glucose solution was added in the position i, ii, iii and iv, 1 mL of 0.5×10^{-7} mM bacteria-mimicking nanoswimmers was subsequently added in the position i, finally the gel containing 1 M glucose was added in the position iii. (B) Absorbance changes of bacteria-mimicking nanoswimmers at different positions within 180 min. (C) Computational simulation showing the diffusion profile of glucose in the microfluidic channel at different time intervals.

enzymatic kinetic, and the value of K_M and V_{MAX} is 34.2 mM and 11.6 μm s^{-1}, respectively.[15] In contrast, negligible activity from PNIPAM@Au particles suggests the effective inhibition of the grafted PNIPAM brushes on the adsorption of GOx during the preparation process at room temperature. Taken together, these results demonstrate the successful preparation of the PNIPAM@JAu@GOx nanoswimmers.

The GOx-catalyzed decomposition of glucose fuels on the asymmetrically distributed GOx side could generate the local gradients of glucose, gluconic acid, and hydrogen peroxide across the nanoswimmers (Figure 2A). To track the trajectory of the PNIPAM@JAu@GOx nanoswimmers with sizes of below 100 nm, the dark-field optical microscopy was conducted. To better record the trajectory of motion, the glycerinum/water mixed solvent (volume ratio: 1:1) was employed to enhance the viscosity of the solvent. Figure 2B illustrates that the average velocity of PNIPAM@JAu@GOx nanoswimmers increased from 1.2 μm s^{-1} at 5 mM glucose solution to 9.1 μm s^{-1} at 80 mM glucose solution, while the concentration of glucose fuels beyond 80 mM had minor influence on the average velocity. By comparison, the JAu@GOx nanoswimmers (without the grafting of polymer brush) exhibit a similar tendency, whereas the velocity is lower than that of PNIPAM@JAu@GOx in the same glucose concentration. The mean square displacement (MSD) of the PNIPAM@JAu@GOx nanoswimmers versus time interval curves show an increased slope in 1 s, suggesting their self-propulsion motion in the presence of glucose fuels (Figure S6).

Since the scattering difference of two faces of the PNIPAM@JAu@GOx nanoswimmers, we further investigated their propulsion behavior by using dynamic light scattering (DLS) measurement according to previous reports.[16] Figure 2C shows that the PNIPAM@JAu@GOx nanoswimmer bestowed a lower rotational diffusion compared with that of the JAu@GOx nanoswimmer. To evaluate the effect of the polymer brushes on the swimming behavior, three types of PNIPAM@JAu@GOx nanoswimmers with different polymer chain lengths were prepared. By tuning the polymerization time, (60 min, 180 min, and 360 min), the length of the grafted PNIPAM brushes on the nanoswimmers are 58.9 ± 1.2 nm, 67.1 ± 0.9 nm, and 89.3 ± 2.1 nm, respectively, as illustrated in Figure S7. We denoted the PNIPAM@JAu@GOx nanoswimmers with 1 h, 3 h, and 6 h polymerization time as PNIPAM@JAu@Gox (1), (2), and (3), respectively. Both the rotational diffusion relaxation times (τ_{rot}, Figure 2D) and the translational relaxation time (τ_{trans}, Figure 2E) of the PNIPAM@JAu@GOx (1, 2, 3) and JAu@GOx nanoswimmers declined with the increasing glucose concentration. Particularly, the longer the grafted polymer chain is, the higher the τ_{rot} of the nanoswimmers is at the same glucose concentration. In contrast, the τ_{trans} of the nanoswimmers with a longer polymer chain has a lower τ_{trans} at the same glucose concentration. For instance, the τ_{rot} of the PNIPAM@JAu@GOx (3) swimmers decreased from 128.7 μs at 0 mM glucose to 86.3 μs at 100 mM glucose, while that of the JAu@GOx nanoswimmers reduced from 105.2 μs at 0 mM glucose to 65.4 μs at 100 mM glucose. And the τ_{trans} of the PNIPAM@JAu@GOx (3) is lower than that of JAu@GOx nanoswimmers (269.2 μs *vs* 315.7 μs with 0 mM glucose, and 194.3 μs to 223.5 μs with 100 mM glucose). Moreover, Figure 2F illustrates that the rotational diffusion coefficient (D_{rot}) of both the PNIPAM@JAu@GOx and JAu@GOx nanoswimmers went up with the increasing glucose concentration and length of polymer brushes, but the D_{rot} of the PNIPAM@JAu@GOx is lower than that of the JAu@GOx. Accordingly, the translational diffusion coefficient D_{trans} of the PNIPAM@JAu@GOx is higher than that of the JAu@GOx nanoswimmers in the same glucose concentration (Figure 2G). The above data reveal that the grafted polymer brushes indeed enhance the translational diffusion, and the PNIPAM@JAu@GOx(3) nanoswimmers display the optimal translation diffusion during the glucose-powered propulsion. It should be attributed that the grafted water-soluble polymer brushes influence the local fluid flow field and thus enhance the self-diffusiophoretic force on the nanoswimmers.

Next, we used the PNIPAM@JAu@GOx(3) as an example to evaluate the effect of polymer brushes on the swimming behavor in depth. The persistence length of the nanoswimmers is estimated by

$$D_{Trans} = D_{Brown} + {}^{l^2}/_{4\tau_{Rot}} \quad (1)$$

$$V = {}^{l}/_{\tau_{Rot}} \quad (2)$$

Where D_{Trans} is translational diffusion coefficient, D_{Brown} is diffusion coefficient of Brownian motion, l is persistence length, and V is velocity.[17] As a result, the persistence length of PNIPAM@JAu@GOx nanoswimmers ranges from 39.1 nm at 0 mM glucose to 54.2 nm at 100 mM glucose, which is higher than that of JAu@GOx nanoswimmers (20.9 nm at 0 mM glucose to 41.8 nm at 100 mM glucose. The ratio of persistence length for the PNIPAM@JAu@GOx to the JAu@GOx reached 1.9 at 10 mM glucose as shown in Figure 2H. Moreover, Figure 2I shows that the ratio of the velocity of the PNIPAM@JAu@GOx to the JAu@GOx nanoswimmers is always beyond 1, and the maximum

10.1002/anie.201907733

ratio of velocity for the PNIPAM@JAu@GOx to JAu@GOx is 2.0 at 10 mM glucose. To further verify the role of polymer brushs on the swimming behavor, a water-soluble polymer, poly(ethylene glycol) dimethacrylate, was grown onto the nanoswimmers (PEGMA@JAu@GOx). The DLS analysis shows that the PEGMA grafted nanoswimmers had similar movement behavior as that of the PNIPAM@JAu@GOx (Figure S8), suggesting that the polymer brush grafting could enhance the translational diffusion of the nanoswimmers, but not limited to the types of water-soluble polymer brushes. Taken together, these data indicates that the polymer brush grafting facilitates efficient directional propulsion of the nanoswimmers through the improvement of their translational diffusion.

Next, we explored whether the PNIPAM@JAu@GOx nanoswimmers exhibited a swarm behavior in the homogenous glucose solution. Since the small size of our nanoswimmers, it is very difficult to directly observe the collective motion and the interaction between individual swimmers by using optical microscopy. In view of this, we monitored the variation of the absorbance of the nanoswimmer suspensions against different time at certain region in the homogenous glucose solution by UV-vis-NIR spectroscopy. The number of nanoswimmers was estimated from the work curve between the absorbance at 530 nm and the number of the predefined nanoswimmer suspensions (Figure S9). We subsequently analyzed the correlation between the standard deviation ΔN with the mean nanoswimmer number <N>. The results illustrate that the nanoswimmers in the absence of glucose shows minor change in ΔN as the increasing number of nanoswimmers (Figure S10A), but the giant number fluctuation in 0.1 M glucose appears once the number of nanoswimmers is beyond 6×10^8 in the observed area, indicating the occurrence of phase separation (Figure S10B). Note that no extra peak in the NIR region, suggesting that the phase separation is not caused by the formation of strong AuNP aggregation during the propulsion. The above data verify that the swarm behavior of the PNIPAM@JAu@GOx nanoswimmers follows a concentration-dependent manner like that of swimming bacteria.[18]

To investigate the chemotactic behavior of the PNIPAM@JAu@GOx nanoswimmers, a three-outlet microfluidic channel was conducted to generate a concentration gradient of glucose fuels at the horizontal plane as illustrated in Figure 3A. The nanoswimmers were injected into the left reservoir (i) of the channel, and a piece of agarose gel containing glucose was put in the right reservoir (iii). The two branched reservoirs (ii and iv) were served as controls. The time-lapse images in Figure S11 shows that the reservoir (iii) appeared a significant number of bright spots after 3 h observed by optical microscopy, suggesting the aggregation of nanoswimmers in this reservoir. In contrast, two branched reservoirs (ii and iv) showed negligible signals. Furthermore, the intensity of different reservoirs in the microfluidic channel was also quantified by using UV-vis-NIR spectra (Figure 3B). It can be seen that only the absorbance in the reservoir (iii) significantly increased. To examine the diffusion profile of glucose during the chemotactic process, the concentration of glucose at different positions from the glucose source with different diffusion times was measured by using high performance liquid chromatography (HPLC) as schematically illustrated in Figure S12A. Figure S12B shows that the concentration of glucose at the positons A, B and C after 30 min is 0.11 M, 0.08 M, and 0.03 M, respectively, indicating the existence of glucose concentration gradient. Based on the experimentally measured results, we theoretically computed the gradient profile of glucose in the microfluidic channel within 180 min according to the time-dependent diffusion equation.[19] The simulated diffusion profile of glucose in Figure 3C shows the existence of the concentration gradient of glucose after 180 min, which is long enough to perform the chemotactic motion of the nanoswimmer swarms along the gradient of glucose during the experiment. In a control experiment, the swimmers without the polymer brushes coating (JAu@GOx) show similar trend of chemotactic motion, but with a lower efficiency (Figure S13). It should be attributed to the lower translational motion of the JAu@GOx swimmer. Taken together, these results demonstrate that a swarm of the PNIPAM@JAu@GOx nanoswimmers actively moved toward the glucose source and exhibited a positively chemotactive behavior along the glucose concentration gradient at the horizontal plane.

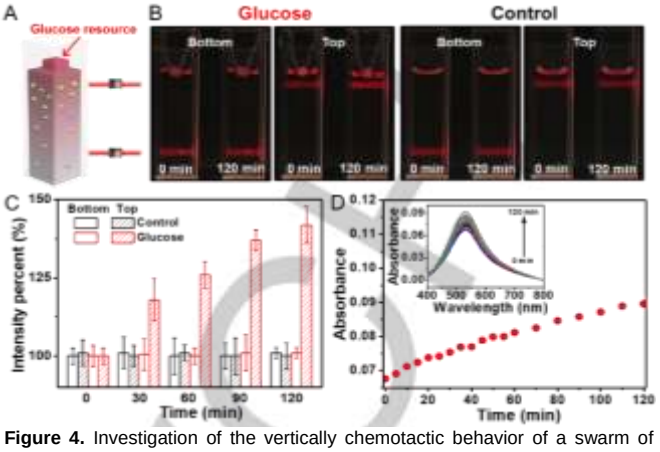

Figure 4. Investigation of the vertically chemotactic behavior of a swarm of bacteria-mimicking PNIPAM@JAu@GOx nanoswimmers. (A) Illustration of the vertical chemotaxis of bacteria-mimicking nanoswimmers toward a gel containing glucose in a cuvette. (B) Time-lapse and (C) intensity percent of nanoswimmers with or without glucose source under the illumination of a light beam for 2 h. (D) Absorbance changes of bacteria-mimicking nanoswimmers at the fixed point in 2 h by utilizing UV-vis-NIR spectroscopy.

To better understand the collective chemotaxis of the PNIPAM@JAu@GOx nanoswimmers under a glucose gradient, we conducted an experiment that a piece of hydrogel containing glucose was put at the top of a 2 mL cuvette containing 4.0 mg nanoswimmers and 15 mM glucose, and then a laser beam with a wavelength of 650 nm was used to illuminate the top and bottom parts of the cuvette as illustrated in Figure 4A. The time-lapse images in Figure 4B show that a red light path appeared when a light beam was irradiated near the bottom part of the cuvette, but the intensity of red light path did not show an obvious change after 2 h. Note that the appearance of the red light path is ascribed to the light scattering of the suspended nanoswimmers (i.e. Tyndall effect), and thus the intensity may be used to qualitatively assess the change of nanoswimmer concentrations. Interestingly, the intensity of red light path close to the glucose resource near the top part of the cuvette obviously improved after 2 h, indicating the

enhanced concentration of nanoswimmers. In control experiments, the intensity of two light paths both at the top and bottom parts of the cuvette without the hydrogel containing glucose resource showed negligible change after 2 h. Such microscale chemotaxis was further quantified by analyzing the intensity of red light. Figure 4C shows that compared with the negligible change of the intensity of various controls, the intensity at the top part of the cuvette increased more than 40% after 2 h, suggesting a directed motion of the nanoswimmers toward the glucose source from the bulk. In view of the fact that the very small size of PNIPAM@JAu@GOx nanoswimmers, it is difficult to directly see individual particles in the swarm. The UV-vis-NIR spectroscopy was thus employed to quantitatively measure the change of their concentration and dispersity since the characteristic adsorption of the monodispersed and aggregated AuNPs.[20] Figure 4D shows that the absorbance intensity of the nanoswimmers at 530 nm on the top part of the cuvette increased as the function of time, indicating the significant accumulation of the nanoswimmers. Given that minor change occurs in the maximum absorption wavelength of 530 nm and no any new absorbance peaks appeared in the NIR region after 2 h (the inset in Figure 4D), it is reasonably deduced that the cluster formation may be neglected. All of nanoswimmers should still remain active and thus form a dynamic swarm during the chemotactic accumulation toward the glucose resource. In addition, the PEGMA@JAu@GOx swimmers also exhibited positively chemotatic motion toward the glucose resource as expected, demonstrating that the chemical composition of water-soluble polymer brushes has less effect on the positive chemotaxis of PB@JAuGOx nanoswimmers (Figure S14). Therefore, these results reveal the positive chemotactic behavior of a swarm of PB@JAu@GOx nanoswimmers along the concentration gradient of glucose fuels.

In summary, we have demonstrated the bacteria-mimicking enzyme-powered nanoswimmers with the enhanced self-propelling motion by the functionalization of polymer brush. These biomimicking nanoswimmer were fabricated by the grafting of polymer brush and glucose oxidase on the opposite surface of gold nanoparticles. The propulsion of the nanoswimmers is driven by the self-diffusiophoresis from the catalytic decomposition of glucose. With elevation of the translational diffusion from the polymer brush functionalization, the resulting bacteria-mimicking nanoswimmers could collectively move toward the glucose resource along the concentration gradient of glucose, and really form a dynamic swarm like those bacteria swarms. Such a macroscale chemotaxis of the nanoswimmer swarms could be utilized for actively seeking the targeted sites, which makes these bacteria-mimicking nanoswimmers appealing for future biomedical applications.

Acknowledgements

We appreciate the help of Prof. Luru Dai for the STROM characterization. This work is financially supported by the National Natural Science Foundation of China (21674029, 21603047, and 21573053), and China Postdoctoral Science Foundation funded project (2016M590286).

Keywords: nanoswimmer • chemotaxis • nanomotor • swarm • enzymatic catalysis

[1] J.-W. Yoo, D. Irvine, D. Discher, S. Mitragotri, *Nat. Rev. Drug Discov.* **2011**, *10*, 521-535.

[2] a) F. Matthäus, M. Jagodič, J. Dobnikar, *Biophys. J.* **2009**, *97*, 946-957; b) U. Alon, M. G. Surette, N. Barkai, S. Leibler, *Nature* **1999**, *397*, 168-171. c) K. K. Dey, S. Das, M. F. Poyton, S. Sengupta, P. J. Butler, P. S. Cremer, A. Sen, *ACS Nano* **2014**, *8*, 11941-11949; d) M. N. Popescu, W. E. Uspal, C. Bechinger, P. Fischer, *Nano Lett.* **2018**, *18*, 5345-5349; e) S. Sengupta, K. K. Dey, H. S. Muddana, T. Tabouillot, M. E. Ibele, P. J. Butler, A. Sen, *J. Am. Chem. Soc.* **2013,** *135*, 1406-1414. f) A. Joseph, C. Contini, D. Cecchin, S. Nyberg, L. Ruiz-Perez, J. Gaitzsch, G. Fullstone, J. Azizi, J. Preston, G. Volpe, G. Battaglia, *Sci. Adv.* **2017**, *3*, e1700362.

[3] a) S. Sanchez, L. Soler, J. Katuri, *Angew. Chem. Int. Ed.* **2014**, *54*, 1414-1444; b) R. Dong, Y. Cai, Y. Yang, W. Gao, B. Ren, *Acc. Chem. Res.* **2018**, *51*, 1940-1947; c) V. V. Singh, J. Wang, *Nanoscale* **2015**, *7*, 19377-19389; d) T. Li, X. Chang, Z. Wu, J. Li, G. Shao, X. Deng, J. Qiu, B. Guo, G. Zhang, Q. He, L. Li, J. Wang, *ACS Nano* **2017**, *11*, 9268-9275; e) W. Gao, X. Feng, A. Pei, Y. Gu, J. Li, J. Wang, *Nanoscale* **2013**, *5*, 4696-4700; f) J. Wang, W. Gao, *ACS Nano* **2012**, *6*, 5745-5751; g) T. Li, A. Zhang, G. Shao, M. Wei, B. Guo, G. Zhang, L. Li, W. Wang, *ACS Nano* **2018**, *28*, 1706066; h) M. Luo, Y. Feng, T. Wang, J. Guan, *Adv. Funct. Mater.* **2018**, *28*, 1706100. i) W. Duan, W. Wang, S. Das, V. Yadav, T. E Mallouk, A. Sen, *Ann. Rev. Anal.Chem.* **2015**, *8*, 311-333.

[4] a) T. Xu, F. Soto, W. Gao, R. Dong, V. Garcia-Gradilla, E. Magaña, X. Zhang, J. Wang, *J. Am. Chem. Soc.* **2015**, *137*, 2163-2166; b) W. Wang, W. Duan, Z. Zhang, M. Sun, A. Sen, T. E. Mallouk, *Chem. Comm.* **2015,** *51,* 1020-1023; c) D. Kagan, S. Balasubramanian, J. Wang, *Angew. Chem. Int. Ed.* **2011,** *50,* 503-506; d) C. Liu, T. Xu, L.-P. Xu, X. J. M. Zhang, *Micromachine* **2017**, *9*, 10.

[5] a) O. Felfoul, M. Mohammadi, S. Taherkhani, D. de Lanauze, Y. Xu, D. Loghin, S. Essa, S. Jancík, D. Houle, M. Lafleur, L. Gaboury, M. Tabrizian, N. Kaou, M. Atkin, T. Vuong, G. Batist, N. Beauchemin, D. Radzioch, S. Martel, *Nat. Nanotechnol.* **2016**, *11*, 941-947; b) B.-W. Park, J. Zhuang, Ö. Yaşa, M. Sitti, *ACS Nano* **2017**, *11*, 8910-8923.

[6] a) A. Solovev, W. Xi, D. H. Gracias, S. Harazim, C. Deneke, S. Sanchez, O. Schmidt, *ACS Nano* **2011**, *6*, 1751-1756; b) J. Li, B. Esteban-Fernández de Ávila, W. Gao, L. Zhang, J. Wang, *Sci. Robot.* **2017**, *2*, eaam6431; c) Y. Mei, A. Solovev, S. Sanchez, O. Schmidt, *Chem. Soc. Rev*. **2011**, *40*, 2109-2119.

[7] R. Liu, A. Sen, *J. Am. Chem. Soc.* **2011**, *133*, 20064-20067.

[8] a) W. Gao, M. D'Agostino, V. Garcia-Gradilla, J. Orozco, J. Wang, *Small* **2013**, *9*, 467-471; b) W. Gao, A. Uygun Oksuz, J. Wang, *J. Am. Chem. Soc*. **2011**, *134*, 897-900; c) F. Mou, C. Chen, H. Ma, Y. Yin, Q. Wu, J. Guan, *Angew. Chem. Int. Ed.* **2013**, *52*, 7208-7212.

[9] T. Xu, F. Soto, W. Gao, V. Garcia-Gradilla, J. Li, X. Zhang, J. Wang, *J. Am. Chem. Soc.* **2014**, *136*, 8552-8555.

[10] a) S. Gaspar, *Nanoscale* **2014**, *6*, 7757-7763; b) X. Ma, A. Hortelão, T. Patiño, S. Sánchez, *ACS Nano* **2016**, *10*, 9111-9122; c) K. K. Dey, X. Zhao, B. M. Tansi, W. J. Méndez-Ortiz, U. M. Córdova-Figueroa, R. Golestanian, A. Sen, *Nano Lett.* **2015**, *15*, 8311-8315; d) M. Nijemeisland, L. K. E. A. Abdelmohsen, W. T. S. Huck, D. Wilson, J. Hest, *ACS Central. Sci.* **2016**, *2*, 843-849. e) T. Patino, A. Porchetta, A. Jannasch, A. Lladó, T. Stumpp, E. Schäffer, F. Ricci, S. Sánchez, *Nano Lett.* **2019** DOI: 10.1021/acs.nanolett.8b04794; f) T. Patiño, X. Arqué, R. Mestre, L. Palacios, S. Sánchez, *Acc. Chem. Res.* **2018**, *51*, 2662-2671.

[11] a) P. Schattling, B. Thingholm, B. Städler, *J. Mater. Chem. A.* **2015**, *27*, 7412-7418; b) P. S. Schattling, M. A. Ramos-Docampo, V. Salgueiriño, B. Städler, *ACS Nano* **2017**, *11*, 3973-3983; c) B. Yameen, A. Farrukh, *Chem.-Asian J.* **2013**, *8*, 1736-1753; d) X. Lin, Q. He, J. Li, *Chem. Soc. Rev.* **2012**, *41*, 3584-3593; e) S. Sengupta, D. Patra, I. Ortiz-Rivera, A. Agrawal, S.

Shklyaev, K. K. Dey, U. Córdova-Figueroa, T. E. Mallouk, A. Sen, *Nat. Chem.* **2014**, *6*, 415-422.

[12] a) X. Ma, A. Jannasch, U.-R. Albrecht, K. Hahn, A. Miguel-López, E. Schäffer, S. Sánchez, *Nano Lett.* **2015**, *15*, 7043-7050. b) H. Muddana, S. Sengupta, T. E Mallouk, A. Sen, P. J Butler, *J. Am. Chem. Soc.* **2010**, *132*, 2110; c) W. Wang, W. Duan, S. Ahmed, T. E. Mallouk, A. Sen, *Nano Today* **2013**, *8*, 531-554.

[13] Q. He, A. Kueller, S. Schilp, F. Leisten, H.-A. Kolb, M. Grunze, J. Li, *Small* **2007**, *3*, 1860-1865.

[14] T. Patiño, N. Feiner-Gracia, X. Arqué, A. Miguel-López, A. Jannasch, T. Stumpp, E. Schäffer, L. Albertazzi, S. Sánchez, *J. Am. Chem. Soc.* **2018**, *140*, 7896-7903.

[15] M. Huo, L. Wang, Y. Chen, J. Shi, *Nat. Commun.* **2017**, *8*, 357.

[16] a) G. Abade, B. Cichocki, M. Ekiel-Jezewska, G. Nägele, E. Wajnryb, J. *Chem. Phys.* **2011**, *134*, 244903; b) M. Glidden, M. Muschol, *J. Phys. Chem. C.* **2012**, *116*, 8128–8137; c) M. Xuan, Z. Wu, J. Shao, L. Dai, T. Si, Q. He, *J. Am. Chem. Soc.* **2016**, *138*, 6492-6497.

[17] T.-C. Lee, M. Alarcón-Correa, C. Miksch, K. Hahn, J. Gibbs, P. Fischer, *Nano Lett.* **2014**, *14*, 2407-2412.

[18] H.-P. Zhang, A. Be'er, E.-L. Florin, H. L. Swinney, *Proc. Natl. Acad. Sci. U. S. A.* **2010**, *107*, 13626-13630.

[19] L. Ramírez-Piscina, *Phys. Rev. E* **2018**, *98*, 013302.

[20] B. Dai, J. Wang, Z. Xiong, X. Zhan, W. Dai, C.-C. Li, S.-P. Feng, J. Tang, *Nat. Nanotechnol.* **2016**, *11*, 1087-1092.

10.1002/anie.201907733

WILEY-VCH

Macroscale Chemotaxis from a Swarm of Bacteria-Mimicking Nanoswimmers

COMMUNICATION

Polymer brush-functionalized glucose oxidase-powered Janus gold nanoswimmers display a swarm chemotaxis toward the glucose resource as natural bacteria.

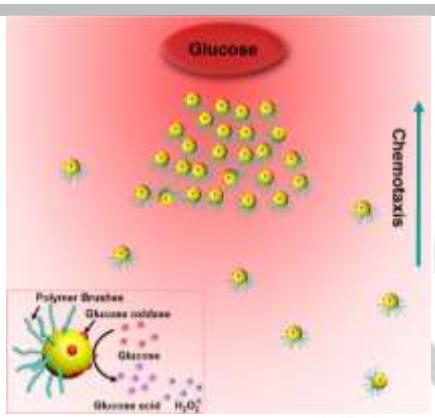

Yuxing Ji, Xiankun Lin, Zhiguang Wu, Yingjie Wu, Wei Gao, and Qiang He

Page 1– Page No.6

Macroscale Chemotaxis from a Swarm of Bacteria-Mimicking Nanoswimmers